ACS OMEGA

Open Access

http://pubs.acs.org/journal/acsodf

Article

Deep and Transfer Learning Approaches for Automated Early Detection of Monkeypox (Mpox) Alongside Other Similar Skin Lesions and Their Classification

Madhumita Pal, Ahmed Mahal,* Ranjan K. Mohapatra,* Ahmad J. Obaidullah, Rudra Narayan Sahoo, Gurudutta Pattnaik, Sovan Pattanaik, Snehasish Mishra, Mohammed Aljeldah, Mohammed Alissa, Mustafa A. Najim, Amer Alshengeti, Bashayer M. AlShehail, Mohammed Garout, Muhammad A. Halwani, Ahmad A. Alshehri, and Ali A. Rabaan*

Cite This: *ACS Omega* 2023, 8, 31747−31757

Read Online

ACCESS | Metrics & More | Article Recommendations | Supporting Information

ABSTRACT: The world faces multiple public health emergencies simultaneously, such as COVID-19 and Monkeypox (mpox). mpox, from being a neglected disease, has emerged as a global threat that has spread to more than 100 nonendemic countries, even as COVID-19 has been spreading for more than 3 years now. The general mpox symptoms are similar to chickenpox and measles, thus leading to a possible misdiagnosis. This study aimed at facilitating a rapid and high-brevity mpox diagnosis. Reportedly, mpox circulates among particular groups, such as sexually promiscuous gay and bisexuals. Hence, selectively vaccinating, isolating, and treating them seems difficult due to the associated social stigma. Deep learning (DL) has great promise in image-based diagnosis and could help in error-free bulk diagnosis. The novelty proposed, the system adopted, and the methods and approaches are discussed in the article. The present work proposes the use of DL models for automated early mpox diagnosis. The performances of the proposed algorithms were evaluated using the data set available in public domain. The data set adopted for the study was meant for both training and testing, the details of which are elaborated. The performances of CNN, VGG19, ResNet 50, Inception v3, and Autoencoder algorithms were compared. It was concluded that CNN, VGG19, and Inception v3 could help in early detection of mpox skin lesions, and Inception v3 returned the best (96.56%) classification accuracy.

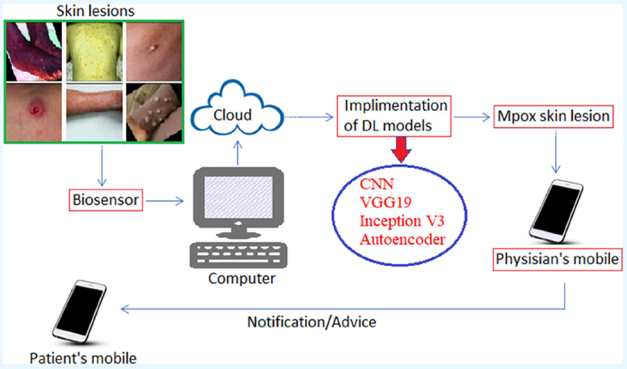

1. INTRODUCTION

Mpox virus that causes monkeypox is a member of the genus orthopoxvirus. It is an enveloped double-stranded DNA virus belonging to family Poxviridae, the same as that of smallpox virus.[1] It was identified in 1958 in monkeys at a Denmark research institute; hence, it is known as the soubriquet Monkeypox.[1,2] The first confirmed human mpox case was reported in 1970 in the Republic of Congo.[1,2] Initially appearing in the African region, it has reached more than 100 nonendemic countries with 84,468 confirmed cases.[3] Mpox is transmitted to humans through close contact with infected individuals or contaminated objects. It has similar symptoms such as chickenpox and measles, which makes it difficult to diagnose. Also, its initial symptoms are similar to COVID-19.[4,5] It commonly circulates in particularly the sexually promiscuous group like gay and bisexuals.[6] The associated social stigma makes its selective vaccination, isolation, and treatment difficult. Recent reports of breakthrough infections and post-vaccine side effects in mpox indicate next-generation novel vaccines.[7]

Although it is usually self-limiting, mpox could be severe in children, pregnant women, or the immunosuppressed (underlying immunodeficiencies may worsen the outcome). Complications include secondary infections, sepsis, encephalitis, bronchopneumonia, and a loss of vision. The incubation period for mpox usually ranges from 5 to 21 days. The invasion is characterized by intense headache, back pain, fever, myalgia, lymphadenopathy, and intense asthenia. Skin eruption begins on days 1−3 of fever. Rashes are developed on the palms of the

Received: April 23, 2023
Accepted: August 9, 2023
Published: August 23, 2023

hands, face, oral mucous membranes, soles of the feet, genitalia, and conjunctivae.

The current 2022 mpox outbreak has now been a concern for healthcare professionals worldwide. Early diagnosis is necessary to counter its rapid progression. An automated IoT-based system to detect mpox is proposed in this study. The data set used was accessed from Mendeley (https://data.mendeley.com/datasets/r9bfpnvyxr). The main objective was to detect and classify mpox skin lesion from other skin lesions like chickenpox, measles, and conventional skin lesion into four classes: Monkeypox, Measles, Chickenpox, and Normal.

The primary objective of the study was to enhance DL-based mpox diagnosis in terms of accuracy, outperforming the algorithms in vogue. The study was envisioned to facilitate a rapid and high-brevity mpox diagnosis. As deep learning promises high-brevity image-based diagnosis, the proposed rapid and fool-proof in silico-integrated IoT and deep learning approach is the novelty of the work. After the general introduction, the rest is organized in the following manner: the related work section provides an overview of the mpox skin lesion image analysis by using deep learning techniques. In the materials and method section, the used data set and methodology are detailed. The adopted system, the methods, and approaches are elaborated. The results and discussion section present the obtained results and an attempt to analyze the same alongside corroborations. The data set adopted for the study was meant for both training and testing, and the performances of CNN, VGG19, Inception v3, and Autoencoder algorithms were analyzed and elaborated in the results and discussion section. Finally, the concluding remarks and possible future extensions of the work are stated.

2. REVIEW OF THE RELATED WORKS

The social, cultural, and economic impacts of a pandemic cannot be ignored. The healthcare infrastructure needs to be equipped well, and the system needs to prepare to deal with such a situation. The lethal impact of the recent mpox is a concern of the international health community. As specific mpox vaccinations or therapies are currently unavailable, early diagnosis seems to be a viable option. Mpox could be diagnosed primarily through a skin lesion test using electron microscopy or polymerase chain reaction (PCR), the more reliable being the latter. PCR has also been effective in the diagnosis of COVID-19 diagnosis. Artificial intelligence (AI)-based techniques through virus image processing and analysis could help in diagnosis. With emerging and more reliable AI models in various domains, such models were proposed for medical image analysis to detect virus-related diseases.[8−101112] Skin diseases like Psoriasis, Vitiligo, Melanoma, Chicken Pox, Ringworm, Lupus, Acne, and Herpes were investigated using deep-learning models.[13] Low-cost image analysis for Herpes Zoster Virus (HZV) detection was proposed using the CNN model with 89.6% accuracy.[14] The transfer learning approach to detect measles was tried recently.[15] The big data approach to detect Ebola virus using an ensemble learning approach by combining artificial neural network (ANN) and genetic algorithm (GA) was proposed.[16] Images of mpox, measles, and chickenpox were analyzed using web mining techniques.[17] A transfer learning approach with the VGG-16 model was evaluated without data augmentation that returned 97% accuracy.[18] There are few reports on detecting mpox. Deep learning shows tremendous promise in image-based diagnosis and could be useful in diagnosing mpox as it invades human skin. This work proposes the use of DL models for the automated early diagnosis of mpox. The performances of the proposed algorithms were evaluated by using the data set available on public domain.

Pramanik et al. proposed an ensemble learning-based framework from a target mpox data set to detect mpox from other skin lesion images.[19] They considered three pretrained base learners Xception, Inception v3, and DenseNet169 to fine-tune the target data set, with an average 93.39% accuracy, 88.91% precision, 96.78% recall, and 92.35% F1 score as returned by their proposed model. Bala et al. evaluated a modified DenseNet-201 deep learning-based CNN model with mpox images data set.[20] The model correctly identified mpox with 93.19 and 98.91% accuracies, using original and augmented data sets, respectively. Yasmin et al. used the data augmentation method to avoid any model "overfitting" and classified monkeypox skin lesion using the poxnet22 DL model with 100% accuracy.[21] Ali et al. detected and classified mpox skin lesion from a data set that contained the images of measles, chickenpox, and mpox skin lesions.[22] They implemented three pretrained DL models ResNet50, VGG-16, and Inception v3 to classify mpox skin lesion from the other two and obtained a maximal accuracy of 82.96% with the ResNet50 model.

Sahin et al. developed an Android mobile application using deep Convolutional Neural Network to detect and classify mpox skin lesion.[23] The CNN model simulation result returned a 91.11% classification accuracy. Sitaula et al. compared 13 different pretrained DL models to detect mpox.[24] Using an ensemble analysis approach, they obtained 87.13% accuracy, 85.44% precision, and 85.40% *F*1-score and AUC with public data set. Ozasahin et al. analyzed four DL models CNN, AlexNet, VGG16 and VGG19 for accurate detection and classification of mpox skin lesion.[25] With 99.60% accuracy, the CNN outperformed, followed by AlexNet (98% accuracy) and VGG16 and VGG19 (80% accuracy). Jaradat et al. used five pretrained DL models VGG16, VGG19, MobileNetV2, ResNet50 and EfficientNetB3 to diagnose mpox skin lesion,[26] and they found that MobileNetv2 model performed the best in terms of accuracy, recall, precision and F1score with 98.16%, 0.96, 0.99, and 0.98 brevity, respectively. Ahsan et al. developed mpox diagnosis model for binary and multiclass classification using Generalization and Regularisation-based Transfer Learning approaches,[27] and tested the model on ten different CNN models. Combined with Xception, the proposed model distinguished with and without mpox cases with 77−88% accuracy. 84−99% accuracy was obtained for multiclass classification using residual network.

3. RESULTS AND DISCUSSION

Various performance metrics were used to measure the performance of the DL models. Each model performance was measured in terms of confusion metrics, accuracy and loss curves, and AUC curve. The numerous parameters used during training are detailed in Table 1. The evaluation of the pretrained classification performance of the DL models is presented in Table 2.

3.1. Comparing the DL Models. The performance of each DL model pretrained for mpox classification was compared based on the performance evaluation data set. The result of the comparison is presented in Table 2. Inception v3 was found to be best performing for mpox (augmented precision = 0.97, recall = 0.96, *F*1-score = 0.97) and for others

https://doi.org/10.1021/acsomega.3c02784
ACS Omega 2023, 8, 31747−31757

Table 1. Numerous Parameters Used in the Performance Evaluation of DL Models

DL models	total parameters	trainable parameters	nontrainable parameters
CNN	1,809,522	1,807,730	1,792
AE	103,936,930	102,760,834	1,176,096
Inception v3	24,572,962	7,918,082	16,654,880
VGG-19	20,027,458	9,441,282	10,586,176
ResNet-50	23,600,002	14,458,370	9,141,632

Table 2. Performance Metrics Comparison of DL Models

	precision	recall	F1-score	support
CNN				
Mpox_augmented	0.95	0.91	0.93	162
others_augmented	0.92	0.96	0.93	158
VGG-19				
Mpox_augmented	0.96	0.92	0.94	162
others_augmented	0.92	0.96	0.94	158
Inception v3				
Mpox_augmented	0.97	0.96	0.97	162
others_augmented	0.96	0.97	0.97	158
AE				
Mpox_augmented	0.89	0.82	0.85	162
others_augmented	0.83	0.89	0.86	158

(augmented precision = 0.96, recall = 0.97, *F*1-score = 0.97), and Autoencoder performed the worst for mpox (augmented precision = 0.89, recall = 0.82, *F*1-score = 0.85) and for others (augmented precision = 0.83, recall = 0.89, *F*1-score = 0.86) among all DL models. It was concluded from Table 2 that the Inception v3 pretrained model was the best among all the DL models in extracting features from medical images and classifying mpox skin lesion from other skin lesions like chickenpox and measles.

3.2. Comparative Analysis in Terms of Confusion Metrics. The confusion matrix for the several models (CNN, VGG19, Inception v3, and Autoencoder) considered is shown in Figure 1. Table 3 shows that Inception v3 outperformed

Table 3. Confusion Matrix Parameter Values

DL model	TP	TN	FP	FN
CNN	148	151	7	14
VGG-19	149	152	6	13
Inception v3	155	154	4	7
Autoencoder	133	141	17	29

others (TP: 155, TN: 154, FP: 4, FN: 7) in classifying mpox skin lesions, as the false negative (FN) and positive values were small compared to other models. The FN value is the most critical among all confusion matrix parameters, as the model

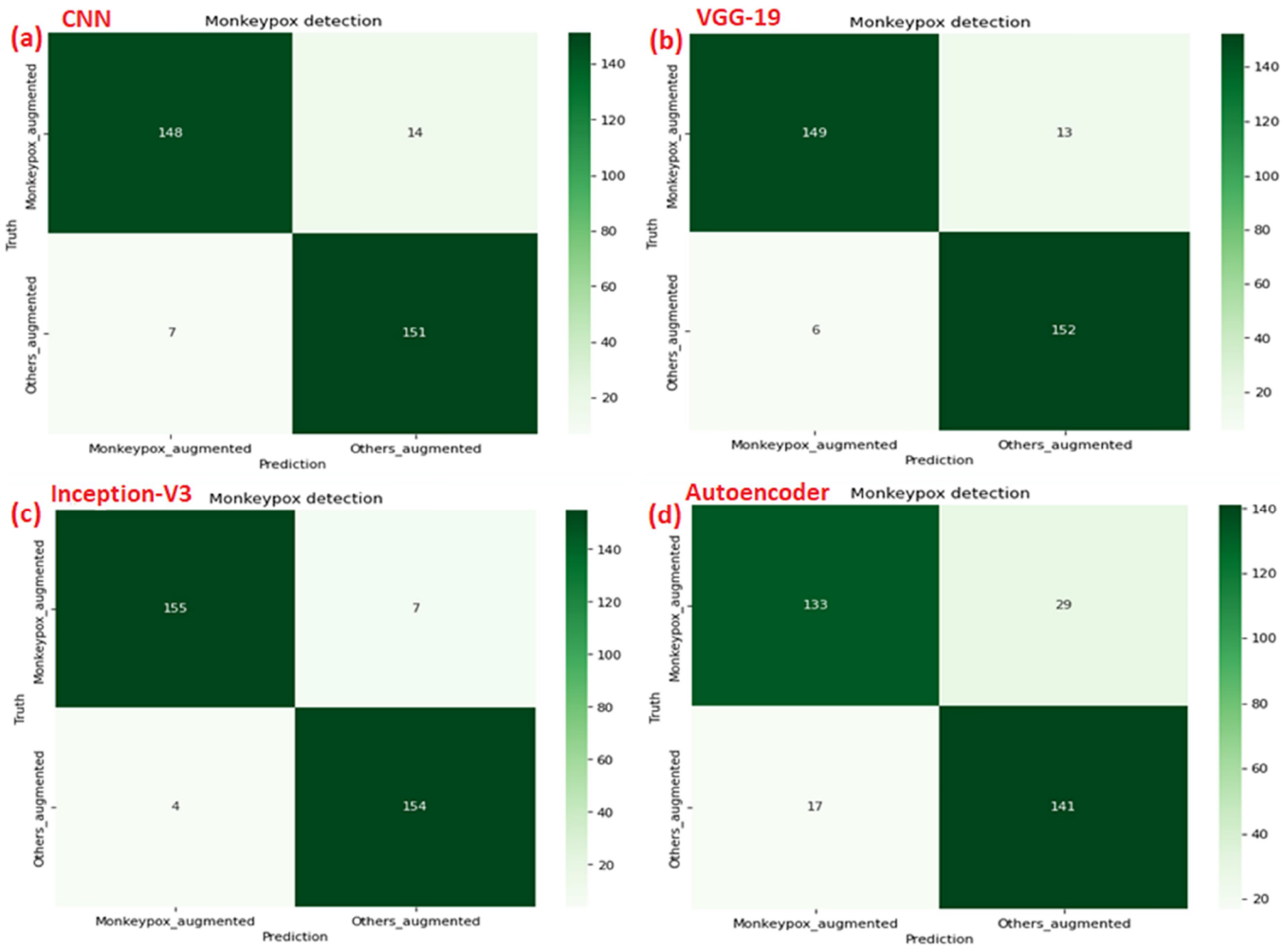

Figure 1. Confusion matrices of (a) CNN, (b) VGG-19, (c) Inception v3. and (d) Autoencoder.

https://doi.org/10.1021/acsomega.3c02784
ACS Omega 2023, 8, 31747−31757

Table 4. Comparison of Accuracy, AUC, and Loss Curve of the Test DL Models

DL model	training accuracy	validation accuracy	training loss	validation loss	training AUC	testing AUC
CNN	99.74	93.43	0.01	0.3	99.91	96.52
VGG-19	99.91	94.06	0.0011	0.45	1	96.96
Inception v3	100.00	96.56	3.95	0.29	1	97.19
Autoencoder	99.96	85.62	0.03	0.39	1	0.92

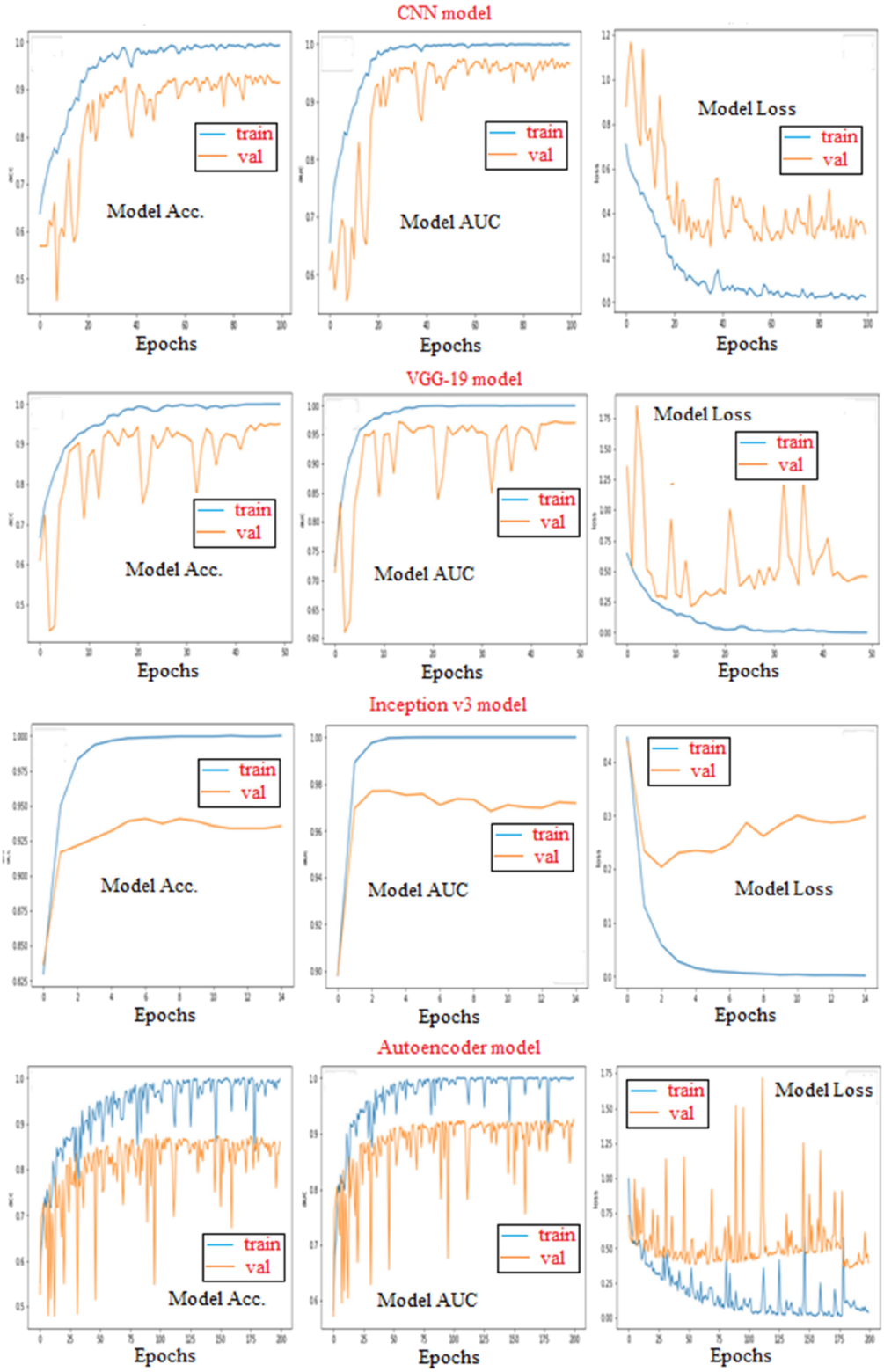

Figure 2. Accuracy, AUC, and loss curve of CNN, VGG-19, Inception v3, and Autoencoder models.

https://doi.org/10.1021/acsomega.3c02784
ACS Omega 2023, 8, 31747−31757

predicts a patient having mpox as not having mpox, which may lead to misdiagnosis and delayed treatment. If the FN value is quite high, it may be life-threatening (Figure 1). The CNN model detected 149 patients with mpox skin lesions and 151 patients with other skin lesions. The model misdiagnosed seven patients as having mpox skin lesions, although they had other skin lesions (FP), and 14 patients as having other skin lesions, although they had mpox skin lesion (FN). Likewise, the VGG-19 model correctly diagnosed 149 patients as suffering from mpox skin lesions and 152 patients as suffering from other skin lesions. The model misdiagnosed six patients with other skin lesions as with mpox skin lesion and 13 patients with mpox skin as with other skin lesions. Autoencoder correctly diagnosed 133 patients with mpox skin lesion and 141 patients with other skin lesions. It misdiagnosed 17 patients with other skin lesions as mpox skin lesions and 29 patients suffering from other skin lesions as having mpox skin lesion. The task of this study was to help clinicians in the early accurate diagnosis of mpox skin lesion by analyzing patient X-rays and advice for early isolation to prevent further transmission. It was okay if a false positive value was received as the patient could be advised to isolate, thereby greatly reducing the risk of chance spread of the virus. The risk would otherwise be high for FN cases (in models with low recall) as the sick remain mobile without isolation, risking further transmission. Inception v3 had 96% recall on the test data set, which proved that it was the best model for the task.

3.3. Comparison of Accuracy. All four test models (CNN, VGG-19, Inception v3, and Autoencoder) showed nearly 100% training accuracy with appreciably high validation accuracy of more than 90% (Table 4). Inception v3 demonstrated the best performance in terms of accuracy, AUC, and minimum loss (training accuracy = 100, testing accuracy = 96.56, training loss = 0.01, validation loss = 0.29, training AUC = 1, testing AUC = 97.19), as also presented in Figure 2. Autoencoder showed the worst performance with a training accuracy of 99.19 and a validation accuracy of 85.62.

3.4. ROC Curve. The ROC curves of the models are shown in Figure 3. The ROC curve measures the diagnosability of a DL model. The more the area under the curve, the more shall be the diagnosis capability of the model. AUC measures the area under the receiver operating characteristics curve. It is a graph between true positives and false positives. The more the value of the area, the better the classification ability of the DL model. Inception v3 had the highest (0.966) area (Figure 3), indicating that it had the maximum classification ability as compared to the other three models for mpox skin lesion.

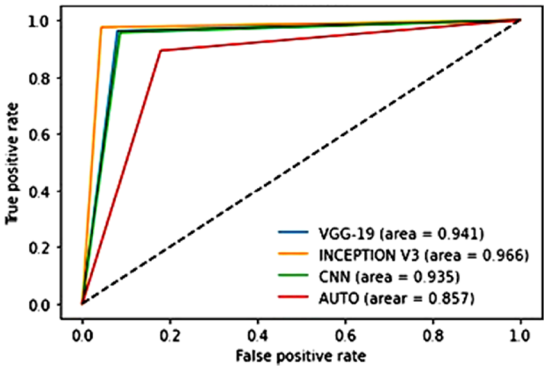

Figure 3. ROC curves for the test DL models.

Figure 3 shows that Inception v3 had the highest (96.6) AUC followed by VGG 19 (94.1), CNN (93.5), and Autoencoder (85.7). A simulation study showed that Inception v3 had the highest diagnosability for mpox, as it had a high (96.6) AUC and Autoencoder contrastingly had the least with the lowest (85.7) AUC value.

3.5. Performance Comparison with Earlier Works. The proposed model was compared with some established documented state-of-the-art methods for mpox classification. Four well-established DL-based methods were used: deep bag of words (BoDVW), attention-based VGG (AVGG), multi-scale deep bag of deep visual words (MBoDVW), and convolutional neural network with long short-term memory (CNNLSTM). The selected optimal hyperparameters from the related papers were considered, and the comparison results are presented in Table 5. The proposed model demonstrated the best performance as compared with other accepted models for mpox virus diagnosis. The results demonstrated that the best performing accurate DL model could be constructed using a combination of transfer learning and data augmentation techniques with VGG16, Resnet50, and Inception v3.

VGG, ResNet50, Inception v3, ResNet18, MobileNet, and Inception v3-based techniques were most frequently employed to build models in earlier investigations. Models employed in this study are standardized in terms of conditions and parameters and are based on transfer learning. CNN, VGG19, Inception v3, and Autoencoder were compared in this study for an expedited and improved model's brevity for use as a real-time assessment tool. The suggested strategy using the Inception v3 model ultimately provided a superior (100%) accuracy level and efficiency compared to other test models.

The accuracy and recall rate of the test models were positive findings in the results. Better results were achieved using the pretrained Inception v3 model for classification tasks, which was also proposed in the simulation work. The data augmentation technique could possibly enhance the accuracy of the Inception v3 model. Data augmentation and data rescaling were used to improve the image quality. The pretrained models were implemented to improve the accuracy and AUC.

Results show that Inception v3 performed better in classifying mpox skin lesions than other mentioned state-of-art models. The finding is encouraging, as it demonstrates the potential of DL applications in early diagnosis. The pretrained model was 100% accurate at classifying mpox and 96.6% accurate in diagnosing with both training and test sets, making it a potentially useful tool for rapid and precise diagnosis in clinical settings.

3.6. Scientific Contribution of the Present Study. The present work primarily contributes to the description of cutting-edge DL methods in detecting mpox early in a real-time system (Figure 5) that was missing in other literature. The speed and accuracy of diagnosis in classifying and diagnosing mpox skin lesion by the proposed model are worth mentioning. Data preprocessing and data augmentation as the two methods used to improve the image classification accuracy of the database before image classification is another aspect. The high degree of classification accuracy (Table 4) of the proposed model with both training and test sets demonstrates that it is a potentially useful tool for rapid and precise diagnosis in clinical settings. This could help doctors/clinicians to make rapid and precise diagnosis of various ailments, improve treatment outcome, and reduce healthcare

https://doi.org/10.1021/acsomega.3c02784
ACS Omega 2023, 8, 31747−31757

Table 5. Performance Comparison of the Proposed with Other Documented Approaches

reference	model	precision	recall	F1-score	accuracy
[22]	Inception v3	0.74	0.81	0.78	74.07
[22]	VGG-19	0.85	0.81	0.83	81.48
[22]	Inception v3	0.74 ± 0.02	0.81 ± 0.07	0.78 ± 0.04	74.07 ± 3.78
[22]	VGG16	0.85 ± 0.08	0.81 ± 0.05	0.83 ± 0.06	81.48 ± 6.87
[22]	ResNet50	0.87 ± 0.07	0.83 ± 0.02	0.84 ± 0.03	82.96 ± 4.57
[23]	ResNet18				86.87
[23]	MobileNetV2				91.11
[24]	Xception	85.01	85.14	85.02	86.51
[24]	Inception v3	82.51	82.30	82.16	84.53
[24]	VGG-19	81.84	81.90	81.03	82.94
[28]	VGG-19	94.36	98.53		97.48
[28]	MobileNet	83.54	95.22		92.30
engaged models	CNN	95	91	93	99.74
	VGG-19	96	92	94	99.91
	Inception v3	97	96	97	100
	Autoencoder	89	82	85	99.96

expenses. The suggested Inception v3 model outperformed other DL-based models in terms of accuracy and efficacy.

Inception v3 could also be a real-time assessment tool and could be deployed on smartphones for real-time detection and predicting mpox instances (Figure 5). Its excellent degree of classification accuracy makes it a potentially useful tool for a rapid, real-time, smart phone-based mpox diagnosis. It is suggested that the proposed model may help classify several skin lesions. Research on automated mpox detection using deep and transfer learning techniques could also potentially pave the way to create new diagnostic approaches for other such diseases. This will help in reducing the challenges in skin lesion diagnosis with accuracy and handle bulk cases, if any, in the future.

However, the study has its limitations too. For instance, the sample size in the data set could be larger. The data set employed here is a purely mpox-dedicated data set without the images of "no skin lesions". Future investigations with bigger data sets that classify different types of skin lesions as well cases without any skin lesion are suggested to be carried out.

4. CONCLUSIONS AND FUTURE PROSPECTS

An automatic diagnostic system for mpox from images was devised in the work using the DL approach. DL models differentiated between mpox skin lesion patients and other skin lesion cases. To implement the DL model, various image enhancement techniques were used to develop a system with improved image quality with the noise eliminated. This article attempted to compare four pretrained DL models on mpox data set. The performance evaluation result of all the DL models showed that Inception v3 was the best with 97.48% precision, 95.67% recall, 96.56% F1-score, and 96.56% accuracy in detecting mpox virus. VGG-19 was the second best model with 96.12% precision, 91.97% recall, 93.99% *F*1-score, and 94.06% accuracy, followed by the CNN model (95.48% precision, 91.35% recall, 93.36% *F*1-score, and 93.43% accuracy). The Autoencoder model performed the least with 88.66% precision, 82.09% recall, 85.24% F1-score, and 85.62% accuracy. Like any scientific work, this one also has limitations, and we propose to state those. First, the data set size was relatively small, so the addition of more data could have a positive effect on the performance. Second, the AI approach was based on pretrained DL models, which may be a problem if these are deployed in memory-constrained settings. Designing lightweight DL models could be useful for a resource-limited scenario. With a unique augmentation approach, the Inception v3 model returned 100% training accuracy and 96.56% validation accuracy, performing at the highest level. As the proposed model achieved a high level of accuracy in classifying mpox, it is a potentially valuable tool for early, automatic, and accurate diagnosis of mpox and other skin lesion diseases like measles, smallpox, chickenpox, and so forth. Studies to demonstrate and validate the model's brevity on bigger image data set may be done in the future. This and the ensuing future studies are anticipated to facilitate early identification, categorization, and management of mpox and other skin lesion ailments. Real-time smart phone-based mpox prediction and diagnosis is a potential extended use of the algorithm, as discussed.

5. MATERIALS AND METHODS

5.1. Data Set Sourcing. Mpox skin lesion image database used in the study were collected from digital sources that included news portals, web resources, and available data in the public domain (https://data.mendeley.com/datasets/r9bfpnvyxr). To remove the bias in the training images such as data preprocessing (the rescaling of images) and augmentation method, two methods were used.

5.2. Data Augmentation. Numerous data augmentation techniques to address the difficulties related to developing an effective classification algorithm are suggested. Rotation, flipping, and zipping augmentation techniques were employed in the study to increase the data set size and prevent overfitting. It broadened the data set and improved the functionality of the model. Data set size could be increased further by using common data augmentation techniques such as zoom, rotation, height shift, shear and width shift ranges, and vertical flip. They enable the production of augmented photos with minor alterations of the original, producing a larger, clear, and clean image.

The final data set contained two directories of augmented images (1428 augmented files of mpox and 1764 of others like chickenpox and measles) and two directories of 228 original images (102 of mpox and 126 of non-mpox cases). The final data set contained 55% non-mpox cases and 45% mpox cases. Low-quality images were discarded through two-stage screen-

https://doi.org/10.1021/acsomega.3c02784
ACS Omega 2023, 8, 31747−31757

Figure 4. Samples of the considered images after data set preprocessing.

ing, and all the images were resized to 224 × 224 × 3; after that, the region of interest is cropped. The considered data set contained augmented images of mpox, chickenpox, and measles with the preliminary objective to categorize mpox

https://doi.org/10.1021/acsomega.3c02784
ACS Omega 2023, 8, 31747−31757

Table 6. Implemented DL Models with Their Advantages and Disadvantages

DL model	advantages	disadvantages
CNN	CNN model automatically extracts the features from the data, without human supervision	As it contains numerous layers, the training time is more
Autoencoder	(1) It is a very efficient deep learning model for learning features from data	Autoencoder requires larger data set to deliver useful output, and the data samples should be clean without "noise"
	(2) It can denoise data and can learn data variation	
ResNet 50	(1) This model has faster training time due to its skip connection	(1) The model is prone to overfitting problem
	(2) More complex function can be learned	(2) Convergence time is more for attending the local minima
	(3) It can reuse activation function of previous layer that helps in reducing the vanishing gradient problem	
Inception v3	It gives high performance by utilizing computing resources efficiently	Requires high computational power to give better result
VGG19	Faster training speed, higher accuracy	The model requires more time to implement

from other skin lesions. Samples of the considered images are shown in Figure 4.

Data augmentation facilitates enhanced accuracy of predicting a model by adding training data, prevents data scarcity, reduces data overfitting, ensures data variability, increases model generalization, and helps resolve class imbalance issues. In this study, tensorflow's image data generator function (IDG) was used to generate augmented images considering the following parameters:

ZOOM_RANGE = [0.99, 1.01]

BRIGHTNESS_RANGE = [0.8, 1.2]

HORZ_FLIP = True(Randomly flip inputs horizontally.)

FILL_MODE = "constant"

5.3. Model Selection and Training. Five DL models (CNN, VGG19, Inception v3, ResNet-50, and Autoencoder) were selected for the study. The architecture and structure for each model were given in Figures S1−S3 and Tables S1−S5. All models were trained using the preprocessed data, and the performances were evaluated and compared in terms of precision, accuracy, recall, and *F*1-score metrics.

5.4. Deep Learning Models Applied in the Study. DL models, autoencoder, convolutional neural network, and pretrained models Inception v3 and VGG-19 available on ImageNet database[29] were applied in the study (Table 6). The pretrained models were used for the purpose of transfer learning.[30] Transfer learning helps to boost the performance of DL models by transferring knowledge from a large data set, while training a small data set. Windows 10 operating system, Tesla K80 GPU, and 12 GB RAM were used to process the data set using Python open-source software. NumPy, Pandas, TensorFlow, Keras, and skLearn Python libraries were used to implement DL models. Google collab and Amazon cloud web services were used to store data. The proposed approach to detect mpox skin lesions is presented in Figure 5.

5.4.1. CNN. CNN is a deep neural network model for feature extraction in image analyses. It reduces the manual job to automatically detect and classify image features. Its architecture consists of primarily three layers, convolutional (input), pooling (output), and fully connected (multiple hidden layers), and uses these layers to extract features from images. Input (convolution) and output (pooling) layers are used to extract features, and the fully connected layer is used to classify. It is mainly used in analyzing clinical images like MRI, CT scan, ultrasound, and so forth.

5.4.1.1. Convolutional Layer. The first layer of CNN architecture is used to detect and extract features from the image, thereby helping in dimension reduction of features. CNN uses a convolution mathematical tool to perform a convolution operation between an input image and a filter with size NXN. The filter is slid across the input image, and the dot product between the filter and the parts of the input image (with respect to filter size; NXN) is obtained. This dot product informs about edges and corners of the image, termed a feature map. After this, the feature map is fed to other layers to decipher other image features.

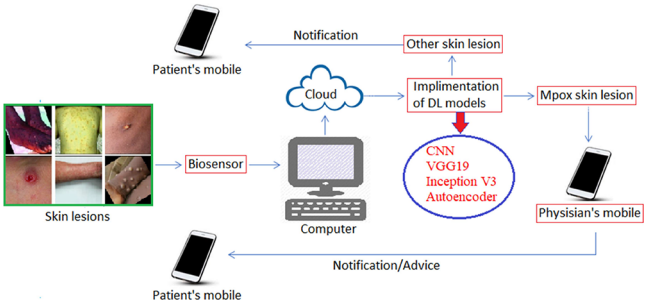

Figure 5. Architecture used in the study: the skin sensor senses the mpox skin lesion, and patient data is stored in the cloud. Then the application data are processed using a digital (computer) platform using python open-source software. Deep learning models are implemented on the mpox skin lesion database to extract the features of the lesion, and then, the DL model classifies the skin lesion as mpox or others. If there is an mpox skin lesion, a notification is sent directly to the clinician's mobile. In case of an emergency, the concerned doctor prescribes medicine to the patient through a mobile app. If it is a skin lesion other than mpox (like chickenpox and measles), then the notification is sent automatically to the patient's mobile and the patient takes therapeutic prescriptions from the doctor accordingly. The cloud system is used to store huge (big) patient data. An "emergency" patient with mpox skin lesion is treated immediately this way without a need to visit a hospital while the misdiagnosis rate is reduced.

5.4.1.2. Pooling Layer. The main objective of this layer is to reduce the dimension of the feature map obtained from the convolutional layer to reduce the computational cost. It is done by reducing the connection between layers and operating on the individual feature map independently. Depending on the manner of features extraction from the feature map, pooling layer may be max, average, or sum.

5.4.1.3. Fully Connected Layer. This FC layer enables an understanding of neural connections between different layers. It contains bias and weights and receives flattened input images. It is a layer present before the output layer, and it initiates image classification.

https://doi.org/10.1021/acsomega.3c02784
ACS Omega 2023, 8, 31747−31757

Table 7. Performance Metrics Formula and Definition of the DL Model

Precision (P)	Recall (R)	F1-score	Accuracy (Acc)	ROC
$\frac{TP}{TP + FP}$	$\frac{TP}{TP + FN}$	$2 \times P \times \frac{R}{P + R}$	$\frac{TP + TN}{TP + TN + FP + FN}$	graph between TPR and FPR; it represents the diagnosis ability of DL models; more the area covered by the curve more will be the diagnosis rate

5.4.1.4. Dropout. This helps in reducing the overfitting problem, which results from the all-neural connection to the fully connected layer. It solves the overfitting problem by dropping the neurons of little relevance randomly from the nodes of the network while training the neural network.

5.4.1.5. Activation Functions. The most significant parameter of the CNN model is the activation function that helps decide the information flow direction and neuron activation in the network. Rectified linear units, TanH, sigmoid, and softmax are the commonly used activation functions used in CNN.

5.4.2. VGG-19. The winner of ImageNet database challenge is a deep CNN model developed by Visual Geometry Group, Oxford University, in 2014 with 19 deep layers trained over millions of images from the ImageNet database. An advance version of VGG-16 consists of 16 convolutional layers, 5 Maxpool layers, and 3 dense layers. It has the ability to classify images into 1000 categories. In the present work, the 224 × 224 × 3 input image size was fed to the VGG-19 model. During the preprocessing phase, the mean of the RGB value of the input image was calculated and subtracted from each image pixel. The whole image was preprocessed using a 3 × 3 kernel size along with stride 1. Spatial padding was used to conserve the resolution of the input image. MaxPooling operation was performed on the reduced feature map of 2 × 2 size to extract image features. Relu activation function was used to add nonlinearity, and sigmoid or TanH was used to reduce the computational time. Three fully connected layers were applied before the output layer, and the SoftMax activation function was used in the final layer for classification.

5.4.3. Inception v3. An advanced version of Inception V1 by GoogleNet, Inception v3 containing 42 wide layers for image classification instead of deep layers was introduced in 2014.[24] It is useful in reducing the overfitting problem that occurs in deep CNN architecture. It is a pretrained model loaded from the ImageNet database with weight and absence of a toplayer. The layers in pretrained Inception v3 model were locked to prevent weight biasing. It uses global average pooling and the Relu activation function to train the network. The last layer for binary classification is the SoftMax classification layer. The global average pooling layer was applied on top of this, followed by 3 layers of 32 dense hidden units with a "Relu" activation function. Finally, the last softMax layer was added with two outputs for the two classes. The model used the Adam optimizer and sparse categorical loss function for compilation.

5.4.4. Autoencoder. It is a type of deep feed-forward neural network wherein the input is the compressed domain representation of latent space, and the output is reconstructed from latent space representation. Its architecture consists of an encoder, hidden layers, and output. Autoencoder is an unsupervised learning model that learns features from its compressed domain representation. The output of the autoencoder is not the same as that of the input due to the loss function (mean square or cross-entropy).

5.5. Performance Evaluation Metrics. Confusion matrix represents the capability of DL models in predicting mpox. One label of confusion matrix represented true value, and another represented the predicted value. The four outputs were TP (true positive), TN (true negative), FP (false positive), and FN (false negative). TP represented doctor diagnosis and model prediction as the same (patient with mpox skin lesion). Doctor's diagnosis report and the model prediction both being false (patient with other skin lesions) were represented by TN. FP represented those where the doctor's diagnosis report was negative (other skin lesions), while the model prediction was positive (with mpox skin lesion), and FN returned the values of positive doctor's diagnosis report (with mpox skin lesion) but negative model prediction (having other skin lesions). The formulas for performance metrics used in the study are provided in Table 7.

5.6. Implementation. The proposed DL model was implemented using Keras (https://github.com/fchollet/keras) in the Python environment using Google Colab (Tensorflow ver. 2.9.2). While applying, the following parameters were tuned: each image was resized to 224 × 224, followed by the online data augmentation as rescale = 1/255, rotation range = 50, width shift range = 0.2, height shift range = 0.2, shear range = 0.25, zoom range = (0.9, 1.01), bright range [0.8, 1.2] and channel shift range = 20. The optimizer was set as "Adam", with 3192 batch size and 0.001 initial learning rate, with binary cross entropy loss function. To prevent overfitting, the learning rate decay over each epoch coupled with the early stopping criteria were utilized. This study used an 80:20::train:test ratio, and the average performance was reported.

■ ASSOCIATED CONTENT

Supporting Information

The Supporting Information is available free of charge at https://pubs.acs.org/doi/10.1021/acsomega.3c02784.

Architecture for different models and structure of different models used in this work (PDF)

■ AUTHOR INFORMATION

Corresponding Authors

Ahmed Mahal − *Department of Medical Biochemical Analysis, College of Health Technology, Cihan University−Erbil, Erbil, Kurdistan Region, Iraq;* orcid.org/0000-0002-6977-3752; Email: ahmed.mahal@cihanuniversity.edu.iq

Ranjan K. Mohapatra − *Department of Chemistry, Government College of Engineering, Keonjhar, Odisha 758 002, India;* orcid.org/0000-0001-7623-3343; Email: ranjank_mohapatra@yahoo.com

Ali A. Rabaan − *Molecular Diagnostic Laboratory, Johns Hopkins Aramco Healthcare, Dhahran 31311, Saudi Arabia; College of Medicine, Alfaisal University, Riyadh 11533, Saudi Arabia; Department of Public Health and Nutrition, The University of Haripur, Haripur 22610, Pakistan;* Email: ali.rabaan@jhah.com

https://doi.org/10.1021/acsomega.3c02784
ACS Omega 2023, 8, 31747−31757

Authors

Madhumita Pal − *Department of Electrical Engineering, Government College of Engineering, Keonjhar, Odisha 758 002, India*

Ahmad J. Obaidullah − *Department of Pharmaceutical Chemistry, College of Pharmacy, King Saud University, Riyadh 11451, Saudi Arabia*

Rudra Narayan Sahoo − *School of Pharmaceutical Sciences, Siksha 'O' Anusandhan (Deemed to be University), Bhubaneswar, Odisha 751 003, India*

Gurudutta Pattnaik − *School of Pharmacy and Life Sciences, Centurion University of Technology and Management, Khordha, Odisha 752 050, India*

Sovan Pattanaik − *School of Pharmaceutical Sciences, Siksha 'O' Anusandhan (Deemed to be University), Bhubaneswar, Odisha 751 003, India;* orcid.org/0000-0003-4610-6647

Snehasish Mishra − *School of Biotechnology, KIIT Deemed-to-be-University, Bhubaneswar, Odisha 751 024, India*

Mohammed Aljeldah − *Department of Clinical Laboratory Sciences, College of Applied Medical Sciences, University of Hafr Al Batin, Hafr Al Batin 39831, Saudi Arabia*

Mohammed Alissa − *Department of Medical Laboratory Sciences, College of Applied Medical Sciences, Prince Sattam bin Abdulaziz University, Al-Kharj 11942, Saudi Arabia;* orcid.org/0000-0002-4045-0810

Mustafa A. Najim − *Department of Medical Laboratories Technology, College of Applied Medical Sciences, Taibah University, Madinah 41411, Saudi Arabia*

Amer Alshengeti − *Department of Pediatrics, College of Medicine, Taibah University, Al-Madinah 41491, Saudi Arabia; Department of Infection prevention and control, Prince Mohammad Bin Abdulaziz Hospital, National Guard Health Affairs, Al-Madinah 41491, Saudi Arabia*

Bashayer M. AlShehail − *Pharmacy Practice Department, College of Clinical Pharmacy, Imam Abdulrahman Bin Faisal University, Dammam 31441, Saudi Arabia*

Mohammed Garout − *Department of Community Medicine and Health Care for Pilgrims, Faculty of Medicine, Umm Al-Qura University, Makkah 21955, Saudi Arabia*

Muhammad A. Halwani − *Department of Medical Microbiology, Faculty of Medicine, Al Baha University, Al Baha 4781, Saudi Arabia*

Ahmad A. Alshehri − *Department of Clinical Laboratory Sciences, College of Applied Medical Sciences, Najran University, Najran 61441, Saudi Arabia*

Complete contact information is available at: https://pubs.acs.org/10.1021/acsomega.3c02784

Author Contributions

All the authors contributed significantly in developing the manuscript. All the authors have reviewed and approved the final draft for submission. M.P., R.K.M., and S.M. have equally contributed and are treated as first authors.

Funding

No funding received.

Notes

The authors declare no competing financial interest.

■ ACKNOWLEDGMENTS

All authors acknowledge and thank their respective affiliations. The authors extend their appreciation to the Researchers Supporting Project number (RSPD2023R620), King Saud University, Riyadh, Saudi Arabia.

■ REFERENCES

(1) Mohapatra, R. K.; Tuli, H. S.; Sarangi, A. K.; Chakraborty, S.; Chandran, D.; Chakraborty, C.; Dhama, K. Unexpected sudden rise of human monkeypox cases in multiple non-endemic countries amid COVID-19 pandemic and salient counteracting strategies: another potential global threat? *Int. J. Surg.* **2022**, *103*, No. 106705.

(2) Mohapatra, R. K.; Kandi, V.; Seidel, V.; Sarangi, A. K.; Mishra, S.; Rabaan, A. A.; Alhumaid, S.; Al Mutair, A.; Dhama, K. Monkeypox lineages amid the ongoing COVID-19 pandemic: A global public health concern. *Int. J. Surg.* **2022**, *107*, No. 106968.

(3) CDC. *2022 Mpox Outbreak Global Map*. 2023. https://www.cdc.gov/poxvirus/monkeypox/response/2022/world-map.html (accessed on February 2023).

(4) Mohapatra, R. K.; Padhi, B. K.; Kandi, V.; Mishra, S.; Rabaan, A. A.; Mohanty, A.; Sah, R. Camel virus (MERS) reported from Qatar: a threat to the FIFA-2022 and Middle East. *QJM: Int. J. Med.* **2022**, No. hcac271.

(5) Sah, R.; Mohapatra, R. K.; Mishra, S.; Chinnam, S.; Rabaan, A. A.; Alshahrani, N. Z.; Mohanty, A.; Al-Ahdal, T.; Leon-Figueroa, D. A.; Padhi, B. K. Cocktail of FIFA 2022 Vis-A-Vis camel beauty pageant championship; potential health threat of MERS among players and fans - A possible global spread. *Travel Med. Infect. Dis.* **2023**, *52*, No. 102541.

(6) Mohapatra, R. K.; Mishra, S.; Kandi, V.; Sarangi, A. K.; Kudrat-E-Zahan, M.; Ali, M. S.; Sahoo, R. N.; Alam, N.; Pattnaik, G.; Dhama, K. Emerging monkeypox cases amid the ongoing COVID-19 pandemic in the Indian subcontinent: A probable healthcare challenge for South East Asia. *Front. Public Health* **2022**, *10*, No. 1066425.

(7) Mohapatra, R. K.; Mishra, S.; Rabaan, A. A.; Mohanty, A.; Padhi, B. K.; Sah, R. Monkeypox breakthrough infections and side-effects: Clarion call for nex-gen novel vaccine. *New Microbe New Infect.* **2023**, *52*, No. 101084.

(8) Sitaula, C.; Shahi, T. B.; Aryal, S.; Marzbanrad, F. Fusion of multi-scale bag of deep visual words features of chest x-ray images to detect covid-19 infection. *Scientifc reports* **2021**, *11*, 23914.

(9) Unnikrishnan, M.; Gontu, H. L.; Khwairakpam, B. S.; Sagar, P. Detection of covid from chest x-rays using gan. *EPRA Int. J. Res. Dev.* **2022**, *7*, 166−175.

(10) Madhavan, M. V.; Khamparia, A.; Gupta, D.; Pande, S.; Tiwari, P.; Hossain, M. S. Res-covnet: An internet of medical health things driven covid-19 framework using transfer learning. *Neural Comput. Appl.* **2021**, 1−14.

(11) Pal, M.; Parija, S.; Mohapatra, R. K.; Mishra, S.; Rabaan, A. A.; Al Mutair, A.; Alhumaid, S.; Al-Tawfiq, J. A.; Dhama, K. Symptom-Based COVID-19 Prognosis through AI-Based IoT: A Bioinformatics Approach. *BioMed. Res. Int.* **2022**, No. 3113119.

(12) Pal, M.; Parija, S.; Panda, G.; Mishra, S.; Mohapatra, R. K.; Dhama, K. COVID-19 prognosis from chest X-ray images by using Deep learning approaches: a next generation diagnostic tool. *J. Pure Appl. Microbiol.* **2023**, *17* (2), 919−930.

(13) Sandeep, R.; Vishal, K.; Shamanth, M.; Chethan, K. Diagnosis of visible diseases using cnns. In *Proceedings of International Conference on Communication and Artifcial Intelligence*; Springer, 2022; pp 459−468.

(14) Lara, J. V. M.; Velásquez, R. M. A. Low-cost image analysis with convolutional neural network for herpes zoster. *Biomed. Signal Process. Control* **2022**, *71*, No. 103250.

(15) Glock, K.; Napier, C.; Gary, T.; Gupta, V.; Gigante, J.; Schafner, W.; Wang, Q. Measles rash identifcation using transfer learning and deep convolutional neural networks. In *2021 IEEE International Conference on Big Data (Big Data)*; IEEE, 2021; pp 3905−3910.

(16) Sarumi, O. A. Machine learning-based big data analytics framework for ebola outbreak surveillance. In *International Conference on Intelligent Systems Design and Applications*; Springer, 2020; pp 580−589.

(17) Ahsan, M. M.; Uddin, M. R.; Farjana, M.; Sakib, A. N.; Momin, K. A.; Luna, S. A. Image data collection and implementation of deep learning-based model in detecting monkeypox disease using modifed vgg16. **2022**. *arXiv [preprint] arXiv:2206.01862*.
(18) Ahsan, M. M.; Uddin, M. R.; Luna, S. A. Monkeypox image data collection. **2022**. *arXiv [preprint] arXiv:2206.01774*.
(19) Pramanik, R.; Banerjee, B.; Efimenko, G.; Kaplun, D.; Sarkar, R. Monkeypox detection from skin lesion images using an amalgamation of CNN models aided with Beta function-based normalization scheme. *PLoS One* **2023**, *18* (4), No. e0281815.
(20) Bala, D.; Hossain, M. S.; Hossain, M. A.; Abdullah, M. I.; Rahman, M. M.; Manavalan, B.; Gu, N.; Islam, M. S.; Huang, Z. MonkeyNet: A robust deep convolutional neural network for monkeypox disease detection and classification. *Neural Networks* **2023**, *161*, 757−775.
(21) Yasmin, F.; Hassan, M. M.; Hasan, M.; Zaman, S.; Kaushal, C.; El-Shafai, W.; Soliman, N. F. PoxNet22: A Fine-Tuned Model for the Classification of Monkeypox Disease Using Transfer Learning. *IEEE Access* **2023**, *11*, 24053−24076.
(22) Ali, S. N.; Ahmed, M. T.; Paul, J.; Jahan, T.; Sani, S. M. S.; Noor, N.; Hasan, T. Monkeypox Skin Lesion Detection Using Deep Learning Models: A Feasibility Study. *arXiv:2207.03342v1 [preprint]* **2022**.
(23) Sahin, V. H.; Oztel, I.; Oztel, G. Y. Human Monkeypox Classification from Skin Lesion Images with Deep Pre-trained Network using Mobile Application. *J. Med. Syst.* **2022**, *46*, 79.
(24) Sitaula, C.; Shahi, T. B. Monkeypox Virus Detection Using Pre-trained Deep Learning-based Approaches. *J. Med. Syst.* **2022**, *46*, 78.
(25) Ozsahin, D. U.; Mustapha, M. T.; Uzun, B.; Duwa, B.; Ozsahin, I. Computer-Aided Detection and Classification of Monkeypox and Chickenpox Lesion in Human Subjects Using Deep Learning Framework. *Diagnostics* **2023**, *13*, 292.
(26) Jaradat, A. S.; Al Mamlook, R. E.; Almakayeel, N.; Alharbe, N.; Almuflih, A. S.; Nasayreh, A.; Gharaibeh, H.; Gharaibeh, M.; Gharaibeh, A.; Bzizi, H. Automated Monkeypox Skin Lesion Detection Using Deep Learning and Transfer Learning Techniques. *Int. J. Environ. Res. Public Health* **2023**, *20*, 4422.
(27) Ahsan, M. M.; Uddin, M. R.; Ali, M. S.; Islam, M. K.; Farjana, M.; Sakib, A. N.; Al Momin, K.; Luna, S. A. Deep transfer learning approaches for Monkeypox disease diagnosis. *Expert Syst. Appl.* **2023**, *216*, No. 119483.
(28) Almutairi, S. A. DL-MDF-OH2: Optimized Deep Learning-Based Monkeypox Diagnostic Framework Using the Metaheuristic Harris Hawks Optimizer Algorithm. *Electronics* **2022**, *11*, 4077.
(29) Deng, J.; Dong, W.; Socher, R.; Li, L. J.; Li, K.; Fei-Fei, L. Imagenet: A large-scale hierarchical image database. In *2009 IEEE conference on computer vision and pattern recognition*; IEEE, 2009; pp 248−255.
(30) Pan, S. J.; Yang, Q. A survey on transfer learning. *IEEE Trans. Knowl. Data Eng.* **2010**, *22* (10), 1345−1359.

https://doi.org/10.1021/acsomega.3c02784
ACS Omega 2023, 8, 31747−31757